Inorganic Chemistry

Communication

Cite This: Inorg. Chem. XXXX, XXX, XXX-XXX

pubs.acs.org/IC

Controlled Dimerization of Mn_{12} Single-Molecule Magnets

Taylor A. Jenkins,[†] Martin Garnero,[†] Sergio A. Corrales,[†] Eric R. Williams,[†] Andrew M. Mowson,[‡] Andrew Ozarowski,[§] Wolfgang Wernsdorfer,[⊥,∥] George Christou,[‡] and Christos Lampropoulos*[,†]

[†]Department of Chemistry, University of North Florida, 1 UNF Drive, Jacksonville, Florida 32224, United States

[‡]Department of Chemistry, University of Florida, Gainesville, Florida 32611, United States

[§]National High Magnetic Field Laboratory (NHMFL), Florida State University, Tallahassee, Florida 32310, United States

[⊥]Physics Institute and Institute of Nanotechnology, Karlsruhe Institute of Technology, 76131 Karlsruhe, Germany

[∥]Institut Nèel, CNRS, 38042 Grenoble, France

Supporting Information

ABSTRACT: Controlled dimerization of Mn_{12} single-molecule magnets (SMMs) was achieved via a synthetic route involving a competition between bridging and terminal ligands, namely, diols and alcohols. The reaction using a 1:1 ratio of the competing ligands resulted in the isolation of a new family of covalently linked dimers of Mn_{12} SMMs. This is the first step toward the controlled growth of SMM oligomeric arrays.

Miniaturization of modern devices necessitates the development of (multi)functional nanomaterials. In addition, the increasing need for computing power for advanced applications has led to the intense investigation of materials for quantum computing. Furthermore, the prospects of ultrahigh-density data storage and molecular spintronics led inorganic chemists to investigate the possibility of using molecular magnets for these applications. All of these prospects constitute motivation for the development of materials based on molecular clusters and single-molecule magnets (SMMs).[1]

SMMs are transition-metal or lanthanide clusters and coordination compounds with appreciable and occasionally high-spin ground states. They are crystalline materials (single crystals) and monodisperse. Another advantage is that they are soluble in organic solvents, and their properties can thus be altered with standard solution chemistry methods.[2] However, their superparamagnetic properties usually become apparent only at liquid-helium temperatures. Even though one goal of researchers in this area is to raise the blocking temperature of these materials, others focus more on the mesoscopic properties that they exhibit [i.e., quantum tunneling of the magnetization (QTM), quantum-phase interference, and entanglement].[1,2] It was previously shown that oligomers of SMMs may exhibit such properties,[3] and thus intentional oligomer formation is of intense interest. Therefore, we report the first successful targeted dimerization of Mn_{12} SMMs.

The first SMM was $[Mn_{12}O_{12}(O_2CMe)_{16}(H_2O)_4]$ (henceforth $Mn_{12}Ac$). The Mn_{12} family holds a special place in the SMM field because of the high symmetry of the magnetic core, the high-spin ground state, the high anisotropy arising from the near-parallel arrangement of the Jahn–Teller axes on Mn^{3+} ions, and others.[4] We have been investigating alcohol exchange on the Mn_{12} core[5] and recently linked the Mn_{12} clusters into the first family of 1D chains using organic diols as bridges.[6]

Once polymerization had been established,[6] we shifted our attention to developing methods to oligomeric products. We hypothesized that an induced competition between the diols (linkers) and monoalcohols (capping agents) could lead to oligomer formation. Furthermore, we used a 1:1 ratio of the two competing ligands to target dimer formation. We chose to investigate cyclohexane–dimethanol ($chdH_2$) linkers, in order to preclude any steric hindrance, and after some preliminary experimentation, we found success using pivalate ligands. Thus, the reaction of preformed $Mn_{12}Ac$ with pivalic acid, $chdH_2$, and the monoalcohol (methanol, MeOH; in a 1:1 ratio with the linker) gave a solution, from which were isolated single crystals of $[Mn_{12}O_{12}(O_2CCMe_3)_{14}(O_2CMe)_2(chdH_2)(MeOH)(H_2O)]_2$ (**1**) suitable for X-ray crystallography.

The structure (Figure 1, top) reveals that two Mn_{12} clusters are linked by the $chdH_2$ linker, and polymerization is capped by two MeOH terminal ligands. The asymmetric unit comprises (a) the Mn_{12} core, namely, a $[Mn_4O_4]^{8+}$ cubane unit at the center of a nonplanar ring of eight Mn^{3+} ions, all bridged by a total of 12 μ_3-O^{2-} ions, (b) 16 carboxylates (14 pivalates/2 acetates), (c) a bridging $chdH_2$, and (d) a terminal MeOH and a terminal water (H_2O; Figure S1).

The Mn^{3+}–Mn^{3+} distance at the point of linkage is ∼10.3 Å, while the mean distance between the cyclohexane rings is ∼10.2 Å. Steric hindrance with the $chdH_2$ groups is likely the reason for the presence of two acetate ligands near the linkers, instead of all of the carboxylates being pivalates. The packing diagram in Figure S2 reveals that this is a site with high electron density, and as such, a mixed-carboxylate $[Mn_{12}]_2$ complex results. Further evidence is provided by the Hirshfield surface analysis of the asymmetric unit in **1**.[7] The Hirshfield surface reveals very short contacts at the areas between the two clusters, which explains the need for a less bulky carboxylate at these spots (Figures 1, bottom, and S3). Moreover, the symmetry-generated dimer is in an anti conformation to minimize inter-Mn_{12} steric hindrance from the carboxylates (Figure 1, middle).

Similar structures were obtained when the reaction was performed using ethanol, 1-propanol, 1-butanol, and 1-pentanol,

Received: October 16, 2017

DOI: 10.1021/acs.inorgchem.7b02640
Inorg. Chem. XXXX, XXX, XXX–XXX

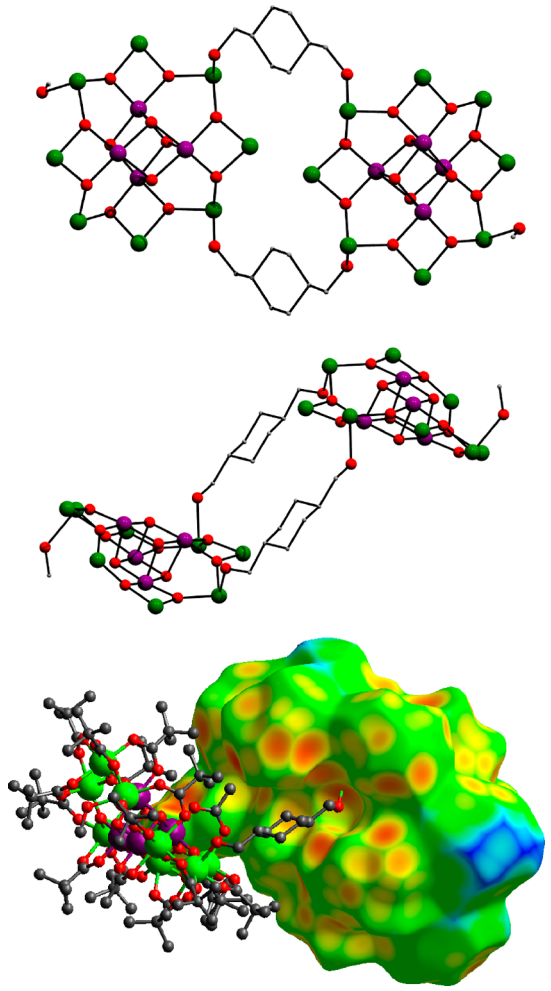

Figure 1. (top) Core structure of **1**, with carboxylate groups and terminal H_2O molecules omitted for clarity. (middle) Side view of the core of **1**, showing the anti conformation of the Mn_{12} units. See Figure S1 for the complete structure. (bottom) Hirshfield surface (d_e) for the asymmetric unit of **1**. The red areas denote small intermolecular contacts, and the blue areas indicate large ones. Color code: Mn^{4+}, purple; Mn^{3+}, green; O, red; C, gray.

albeit the isolated yields and crystal quality were significantly lower for these analogues. Figure 2 shows the structure of complex Core structure of $[Mn_{12}O_{12}(O_2CCMe_3)_{14}(O_2CCH_3)_2(chdH_2)(PrOH)(H_2O)]_2$ (**2**), the 1-propanol analogue (emphasized with orange bonds).[7] The Mn^{3+}–Mn^{3+} distance at the bridging site is similar to that of **1**, namely, 10.3 Å, and the mean distance between the cyclohexane rings is also 10.3 Å. The core is not altered, with nearly identical bond angles and distances. It is thus evident that the identity of the terminal ligands does not significantly affect the overall structure of the Mn_{12} dimer.

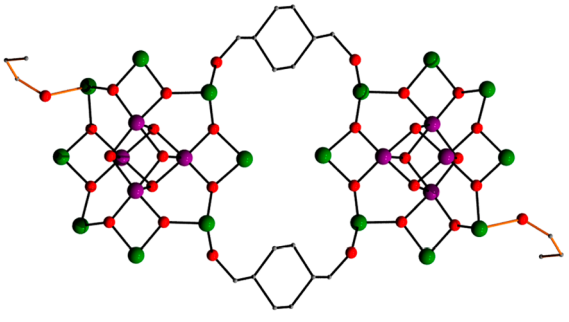

Figure 2. Core structure of **2**, with carboxylates and terminal H_2O molecules omitted for clarity. Color code: Mn^{4+}, purple; Mn^{3+}, green; O, red; C, gray.

Magnetic susceptibility studies were performed on a microcrystalline sample of **1**. The direct-current (dc) magnetic susceptibility revealed features typical in Mn_{12} SMMs, namely, a combination of ferro- and antiferromagnetic interactions and a ground state of S = 10 (Figure S4). No significant exchange interaction between the two Mn_{12} units was evident in the dc studies, as no significant drop in the susceptibility was observed at the lowest temperatures. This was to be expected because of the $chdH_2$ linker, which does not have a continuous π system to facilitate superexchange. In previous studies of SMM oligomers, this was accomplished using carboxylates, carbamates, oximes, and azides.[8] Thus, as expected for **1**, no communication between the Mn_{12} units was observed in data at ≥5.0 K. This is also corroborated by the in-phase alternating-current (ac) studies, which confirm an S = 10 ground state. The out-of-phase ac studies (Figure S5) reveal superparamagnetic properties for the complex, with frequency-dependent peaks signifying SMM behavior. It is also noted that there is no evidence of fast-relaxing species present in this sample.[9]

Magnetization hysteresis studies were performed on single crystals of **1** using a μ-SQUID. The coercivity increases with decreasing temperature and increasing field sweep rates, while characteristic steps were also observed (Figure 3) because of QTM, which is typical of many SMMs. Figure 3B shows a derivative spectrum of the hysteresis study. The peaks appear to

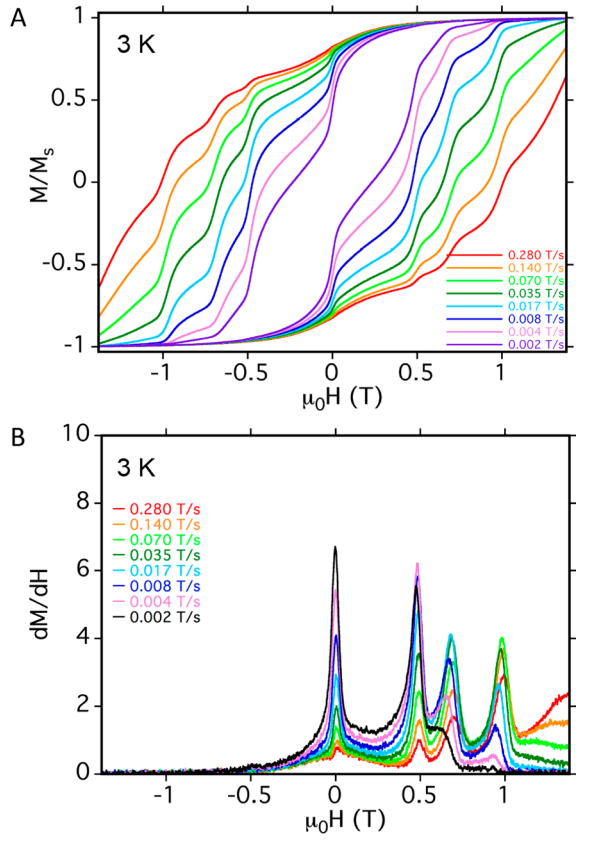

Figure 3. (A) Isothermal magnetization hysteresis loops at 3.0 K. (B) First derivative plot.

DOI: 10.1021/acs.inorgchem.7b02640
Inorg. Chem. XXXX, XXX, XXX−XXX

be superimposed with the first step at zero magnetic field, which affirms the absence of exchange-bias effects, even those originating through space (i.e., dipole−dipole interactions). One thing that is noticeable, however, is the variable size of the QTM steps and their irregular spacing. This is partially due to the crystal packing of the material, where dimers are present in two different orientations. This necessitated the field to be aligned in an intermediate orientation, which explains the irregularity in the spacing of the QTM steps (Figure 3B).

In order to measure the zero-field-splitting parameter D and to be able to compare it to previously reported values for Mn_{12} polymeric chains[6] and Mn_{12} monomers,[3] high-frequency/high-field electron paramagentic resonance (HFEPR) measurements were performed on microcrystalline samples of **1** and **2** (Figure S6). The fitting was performed using the Hamiltonian in eq 1, using parameters from Table 1 and $B_4^0 = -2.0 \times 10^{-5}$ cm^{-1}. The results are summarized in Table 1.

$$\hat{H} = D\hat{S}_z^{\,2} + B_4^0\hat{O}_4^0 + \mu_B BgS \quad (1)$$

Table 1. HFEPR Results for Complexes 1 and 2

	g_x/g_y	g_z	D (cm^{-1})
1	1.875	1.965	−0.467
2	1.921	1.910	−0.464

The data revealed that **1** and **2** exhibit nearly identical D values, which is consistent with the previously identified trend of the D values being dependent upon the distance between the Mn_{12} units (in both **1** and **2**, the $Mn^{3+} - Mn^{3+}$ distance at the linkage site is 10.3 Å).[6] In addition, the D values of **1** and **2** appear to be lower than those of the Mn_{12} polymeric chains in which the easy axes are oriented parallel to the chain direction and slightly higher than the chain where the easy axes are perpendicular to the length of the chain (see Figure S7).[6] Because in complexes **1** and **2** the easy axes of the Mn_{12} units are in an intermediate orientation, the HFEPR results are consistent with the structural features of the materials. Thus, we have identified a new trend in these linked Mn_{12} systems, where the D value appears to depend on the easy axis orientation as opposed to the direction of the oligomer or polymer formation.

In conclusion, the rational synthesis of the first dimeric species based on Mn_{12} SMMs is reported. Complex **1** was characterized using structural and physical methods, which revealed the absence of inter-Mn_{12} exchange interactions. Through the HFEPR study, we also uncovered a new trend in the structure−property relationship of linked Mn_{12} systems, where the HFEPR-measured D value appears to be consistently dependent on the relative orientation of the Mn_{12} easy axis with the linkage direction. In the synthesis of **1**, the diol/alcohol ratio was 1:1, which was also retained in the ligand ratio on the asymmetric unit. This deliberate linker/terminal ligand ratio led to the formation of a dimer in a highly controlled manner. This constitutes proof-of-principle for our synthetic approach. The competing-ligand methodology has so far produced a number of dimeric analogues and represents a promising future route to higher oligomers. Furthermore, it is hypothesized that a priori variation of the linker-to-terminal ligand ratio will lead to oligomers of targeted size.

■ ASSOCIATED CONTENT

Supporting Information

The Supporting Information is available free of charge on the ACS Publications website at DOI: 10.1021/acs.inorgchem.7b02640.

Experimental and measurement details, additional figures, magnetism studies, and HFEPR results (PDF)

Accession Codes

CCDC 1580062 contains the supplementary crystallographic data for this paper. These data can be obtained free of charge via www.ccdc.cam.ac.uk/data_request/cif, or by emailing data_request@ccdc.cam.ac.uk, or by contacting The Cambridge Crystallographic Data Centre, 12 Union Road, Cambridge CB2 1EZ, UK; fax: +44 1223 336033.

■ AUTHOR INFORMATION

Corresponding Author

*E-mail: c.lampropoulos@unf.edu.

ORCID

Andrew Ozarowski: 0000-0001-6225-9796

George Christou: 0000-0001-5923-5523

Christos Lampropoulos: 0000-0001-9065-1453

Notes

The authors declare no competing financial interest.

■ ACKNOWLEDGMENTS

C.L. thanks the Research Corp., Dreyfus Foundation, and National Science Foundation (NSF; Grants DMR-1429428 and DMR-1626332 to C.L. and Grant CHE-1565664 to G.C.). W.W. thanks the Alexander von Humboldt Foundation. The NHMFL is funded by the NSF (Grant DMR-1157490) and the State of Florida. Dr. Bruce Noll (Bruker AXS Inc.) is acknowledged for his help with the challenging crystal structures.

■ REFERENCES

(1) (a) Bogani, L.; Wernsdorfer, W. *Nat. Mater.* **2008**, *7*, 179−186. (b) Affronte, M.; Troiani, F. In *Molecular magnets: Physics and Applications*; Bartolome, S. J., Luis, F., Fernandez, J. F., Eds.; Springer: Heidelberg, Germany, 2013; pp 249−270.

(2) (a) Christou, G. Single-Molecule Magnets: A Molecular Approach to Nanoscale Magnetic Materials. *Polyhedron* **2005**, *24*, 2065−2075. (b) Aromi, G.; Brechin, E. K. In *Single-molecule magnets and related phenomena*; Winpenny, R., Ed.; Springer: Heidelberg, Germany, 2006; pp 1−67. (c) Friedman, J. R.; Sarachik, M. P. Single-molecule nanomagnets. *Annu. Rev. Condens. Matter Phys.* **2010**, *1*, 109−128.

(3) (a) Nguyen, T. N.; Wernsdorfer, W.; Shiddiq, M.; Abboud, K. A.; Hill, S.; Christou, G. Supramolecular Aggregates of Single-Molecule Magnets: Exchange-biased Quantum Tunneling of Magnetization in a Rectangular $[Mn_3]_4$ Tetramer. *Chem. Sci.* **2016**, *7*, 1156−1173. (b) Pineda, E. M.; Lan, Y.; Fuhr, O.; Wernsdorfer, W.; Ruben, M. Exchange-bias quantum tunnelling in a CO_2-based Dy_4-single molecule magnet. *Chem. Sci.* **2017**, *8*, 1178−1185. (c) Nava, A.; Rigamonti, L.; Zangrando, E.; Sessoli, R.; Wernsdorfer, W.; Cornia, A. Redox-Controlled Exchange Bias in a Supramolecular Chain of Fe_4 Single-Molecule Magnets. *Angew. Chem.* **2015**, *127*, 8901−8906.

(4) Bagai, R.; Christou, G. The Drosophila of Single-Molecule Magnetism: $[Mn_{12}O_{12}(O_2CR)_{16}(H_2O)_4]$. *Chem. Soc. Rev.* **2009**, *38*, 1011−1026.

(5) (a) Lampropoulos, C.; Redler, G.; Data, S.; Abboud, K. A.; Hill, S.; Christou, G. Binding of Higher Alcohols onto Mn_{12} Single-Molecule Magnets (SMMs): Access to the Highest Barrier Mn_{12} SMM. *Inorg. Chem.* **2010**, *49*, 1325−1336. (b) Lampropoulos, C.; Murugesu, M.; Harter, A. G.; Wernsdofer, W.; Hill, S.; Dalal, N. S.; Reyes, A. P.; Kuhns,

DOI: 10.1021/acs.inorgchem.7b02640
Inorg. Chem. XXXX, XXX, XXX−XXX

P. L.; Abboud, K. A.; Christou, G. Synthesis, Structure, and Spectroscopic and Magnetic Characterization of $[Mn_{12}O_{12}(O_2CCH_2Bu^t)_{16}(MeOH)_4]\cdot MeOH$, a Mn_{12} Single-Molecule Magnet with True Axial Symmetry. *Inorg. Chem.* **2013**, *52*, 258−272. (c) Harter, A. G.; Lampropoulos, C.; Murugesu, M.; Kuhns, P.; Reyes, A.; Christou, G.; Dalal, N. S. ^{55}Mn Nuclear Spin Relaxation in the Truly Axial Single-Molecule Magnet Mn_{12}-^{t}-butylacetate Thermally Activated down to 400 mK. *Polyhedron* **2007**, *26*, 2320−2324.

(6) Corrales, S. A.; Cain, J. M.; Uhlig, K. A.; Mowson, A. M.; Papatriantafyllopoulou, C.; Peprah, M. K.; Ozarowski, A.; Tasiopoulos, A. J.; Christou, G.; Meisel, M. W.; Lampropoulos, C. Introducing Dimensionality to the Archetypical Mn_{12} Single-Molecule Magnet: a Family of $[Mn_{12}]_n$ Chains. *Inorg. Chem.* **2016**, *55*, 1367−1369.

(7) See the Supporting Information for more details.

(8) (a) Spackman, M. A.; Byrom, P. G. A novel definition of a molecule in a crystal. *Chem. Phys. Lett.* **1997**, *267*, 215−220. (b) McKinnon, J. J.; Spackman, M. A.; Mitchell, A. S. Novel tools for visualizing and exploring intermolecular interactions in molecular crystals. *Acta Crystallogr., Sect. B: Struct. Sci.* **2004**, *60*, 627−668. (c) Hirshfeld, F. L. Bonded-atom fragments for describing molecular charge densities. *Theor. Chim. Acta* **1977**, *44*, 129−138.

(9) (a) Chakov, N. E.; Lee, S. C.; Harter, A. G.; Kuhns, P. L.; Reyes, A. P.; Hill, S. O.; Dalal, N. S.; Wernsdorfer, W.; Abboud, K. A.; Christou, G. The Properties of the $[Mn_{12}O_{12}(O_2CR)_{16}(H_2O)_4]$ Single-Molecule Magnets in Truly Axial Symmetry: $[Mn_{12}O_{12}(O_2CCH_2Br)_{16}(H_2O)_4]\cdot 4CH_2Cl_2$. *J. Am. Chem. Soc.* **2006**, *128*, 6975−6989. (b) Aubin, S. M. J.; Sun, Z.; Eppley, H. J.; Rumberger, E. M.; Guzei, I. A.; Folting, K.; Gantzel, P. K.; Rheingold, A. L.; Christou, G.; Hendrickson, D. N. Single-Molecule Magnets: Jahn-Teller Isomerism and the Origin of Two Magnetization Relaxation Processes in Mn_{12} Complexes. *Inorg. Chem.* **2001**, *40*, 2127−2146. (c) Inglis, R.; Bendix, J.; Brock-Nannestad, T.; Weihe, H.; Brechin, E. K.; Piligkos, S. Frozen-solution magnetisation dynamics of hexanuclear oxime-based Mn^{III} Single-Molecule Magnets. *Chem. Sci.* **2010**, *1*, 631−636. del Carmen Giménez-López, M.; Moro, F.; La Torre, A.; Gómez-García, C. J.; Brown, P. D.; van Slageren, J.; Khlobystov, A. N. Encapsulation of single-molecule magnets in carbon nanotubes. *Nat. Commun.* **2011**, *2*, 407.

DOI: 10.1021/acs.inorgchem.7b02640
Inorg. Chem. XXXX, XXX, XXX−XXX